Journal of Materials Chemistry C

ROYAL SOCIETY OF CHEMISTRY

COMMUNICATION

View Article Online
View Journal | View Issue

Cite this: J. Mater. Chem. C, 2023, 11, 8002

Received 19th January 2023,
Accepted 27th March 2023

DOI: 10.1039/d3tc00236e

rsc.li/materials-c

Porous film impregnation method for record-efficiency visible-to-UV photon upconversion and subsolar light harvesting†

Naoyuki Harada,[a] Masanori Uji,[a] Baljeet Singh,[a] Nobuo Kimizuka *[ab] and Nobuhiro Yanai *[abc]

Photon upconversion from visible light to ultraviolet (UV) light is useful for various photochemical reactions such as artificial photosynthesis, but its efficiency is low under practical film conditions. Here, we demonstrate a film with a record-high visible-to-UV upconversion efficiency of 27.6% by simply soaking a porous film with a low-volatile upconversion solution. Furthermore, by combining this film with a microlens array, a significantly low threshold excitation light intensity of less than 0.60 mW cm^{-2}, at least one order of magnitude lower than solar irradiance, is achieved.

10th Anniversary Statement

Congratulations to the *Journal of Materials Chemistry A*, *B*, and *C* on a decade filled with success. These journals have been a very important home for our photochemistry community, as evidenced by the many high quality and timely papers that have been continuously published. It is also worth mentioning that these journals have contributed greatly to the development of our community in various ways, such as special issues, events, and recognitions. Coincidentally, I (Nobuhiro Yanai) also started my academic career in Japan 10 years ago, and I have had the privilege of sharing in the growth of these journals, publishing 7 papers, serving as a guest editor of the themed collection "Materials for thermally activated delayed fluorescence and/or triplet fusion upconversion", and being selected as one of the Emerging Investigators 2021. There is no doubt that materials have the power to open new frontiers of science and solve society's problems, and I wish the *Journal of Materials Chemistry* family continued success while supporting the future development of materials chemistry.

Introduction

Triplet–triplet annihilation-based photon upconversion (TTA-UC) can utilize low-energy photons to produce higher-energy photons at a weak excitation light intensity.[1–19] TTA-UC is usually composed of two types of chromophores: triplet donors (sensitizers) and acceptors (emitters) (Fig. 1a). The general TTA-UC mechanism begins with light absorption by the donor. The generated excited singlet state of the donor ($S_{1,D}$) transforms to an excited triplet state ($T_{1,D}$) by intersystem crossing (ISC), followed by triplet energy transfer (TET) from the donor to the acceptor. The sensitized acceptor triplets ($T_{1,A}$) annihilate, generating the higher energy excited singlet state of the acceptor ($S_{1,A}$). The final process yields upconverted emission with energy higher than the donor absorption.

TTA-UC chromophores that convert visible light to ultraviolet (UV) light ($\lambda < 400$ nm) have been extensively studied.[20–38] It is applicable to a wide range of photochemical reactions, including solar hydrogen production.[29,39–41] While the efficiency of visible-to-UV TTA-UC has been limited to below 10% for several years due to the absence of an appropriate UV acceptor with a low T_1 energy level, recent research efforts to find better chromophores have brought great advances. For example, we have reported a high visible-to-UV TTA-UC efficiency η_{UC} (theoretical maximum: 100%) over 20% by developing a solution system of Ir coumarin complex ($Ir(C6)_2(acac)$) and 1,4-bis((triisopropylsilyl)ethynyl)naphthalene (TIPS-Nph) as the donor and the acceptor, respectively.[33,34] Albinsson and coworkers have reported the highest visible-to-UV TTA-UC efficiency of 26.2% by combining TIPS-Nph with a TADF-type sensitizer 4CzBN in solution.[36] Wenger and Kerzig *et al.* have utilized a couple of visible-to-UV upconverting chromophores for challenging photoreactions.[29]

[a] *Department of Applied Chemistry, Graduate School of Engineering, Kyushu University, 744 Moto-oka, Nishi-ku, Fukuoka 819-0395, Japan. E-mail: yanai@mail.cstm.kyushu-u.ac.jp, n-kimi@mail.cstm.kyushu-u.ac.jp*

[b] *Center for Molecular Systems (CMS), Kyushu University, 744 Moto-oka, Nishi-ku, Fukuoka 819-0395, Japan*

[c] *FOREST, JST, 4-1-8 Honcho, Kawaguchi, Saitama 332-0012, Japan*

† Electronic supplementary information (ESI) available: Experimental details, transmittance of solvents, TTA-UC results of a solution, absorption and fluorescence spectra, SEM images, thicknesses of porous films, TGA curves, upconverted photoluminescence intensities for one hour, and threshold excitation light intensity. See DOI: https://doi.org/10.1039/d3tc00236e

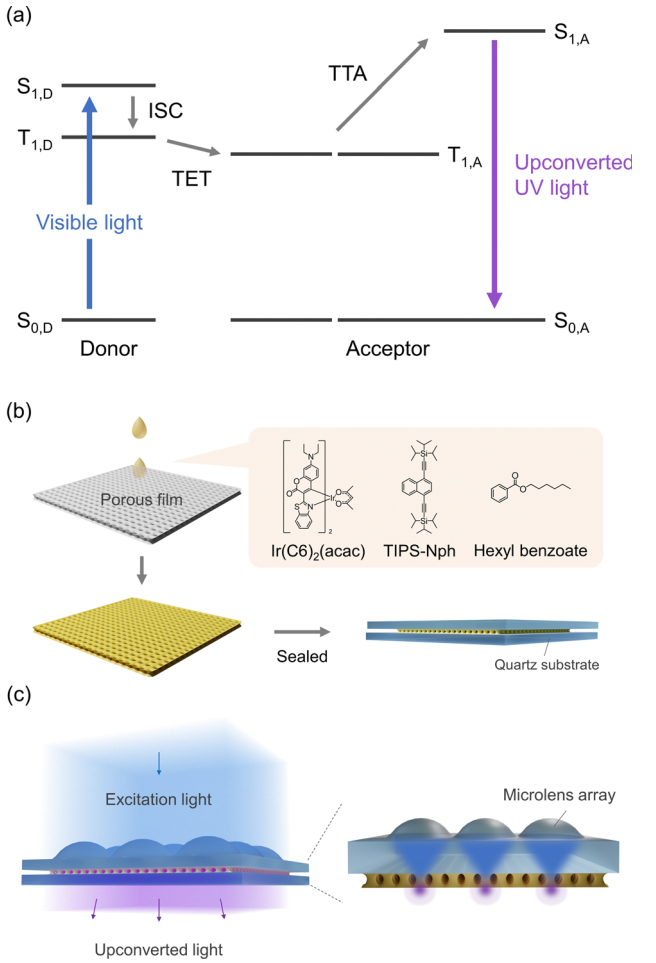

Fig. 1 (a) Typical mechanism of TTA-UC. (b) Schematic illustration of porous film impregnation method using $Ir(C6)_2(acac)$, TIPS-Nph, and hexyl benzoate as a donor, acceptor and solvent, respectively. (c) Schematic illustration of integrating a porous film with a microlens array.

For practical applications of TTA-UC, it is particularly desirable to achieve TTA-UC in the form of films.[25,42–46] However, the examples of films showing visible-to-UV TTA-UC have been limited, and only modest efficiency was reported, such as 2.6% in a polyurethane film containing Ir(ppy-DBP) and a pyrene derivative (DBP) by Ma *et al.* and 8.6% in neat PPO doped with CBDAC reported by Murakami *et al.*[25,28,47,48] By implementing recently-discovered new chromophores, it is expected to boost the visible-to-UV TTA-UC efficiency of the films as well.

Here, we report the highest visible-to-UV TTA-UC efficiency of 27.6% as a film. We developed a simple porous film impregnation method where an upconverting low-volatile solution is introduced into a porous film and sealed with quartz substrates (Fig. 1b). Hexyl benzoate was used as the low-volatile solvent to exhibit excellent TTA-UC properties by Weder and Monguzzi *et al.*[49] TIPS-Nph and $Ir(C6)_2(acac)$ were used as upconverting chromophores. The resulting film showed the highest visible-to-UV TTA-UC efficiency of 27.6% by preserving the good performance of the solution and reducing the inner filter effect. Furthermore, by combining this film with a microlens array, the threshold excitation light intensity (I_{th}) became less than 0.60 mW cm^{-2}, much lower than the sunlight intensity (Fig. 1c).

Results and discussion

We first studied the TTA-UC properties of the bulk solution of TIPS-Nph and $Ir(C6)_2(acac)$ in hexyl benzoate. Hexyl benzoate is a low-volatile solvent with a boiling point above 200 °C[50] and showed a high transmittance in the wavelength region above 350 nm (Fig. S2, ESI†). Upon irradiation of a laser, the deaerated hexyl benzoate solution of TIPS-Nph and $Ir(C6)_2(acac)$ showed an upconverted emission in the UV region below 400 nm (Fig. S3a, ESI†). The TTA-UC efficiency η_{UC} was found to be 16.7% at 7.0 W cm^{-2} by a relative method using the hexyl benzoate solution of coumarin 6 as a standard (Fig. S3b, ESI†), which is close to the previously reported value of 20.5% in a THF solution of the same donor–acceptor pair.[33]

The TTA-UC efficiency can be expressed by the following equation,[7]

$$\eta_{UC} = f\Phi_{ISC}\Phi_{TET}\Phi_{TTA}\Phi_F \quad (1)$$

where f is the spin statistical factor, Φ_{ISC}, Φ_{TET}, Φ_{TTA}, and Φ_F are the efficiencies of ISC, TET, TTA, and acceptor fluorescence, respectively. In the current system, Φ_{ISC} and Φ_{TTA} can be approximated by 100% because the donor fluorescence was not observed, and the TTA-UC efficiency was estimated at an excitation light intensity well above I_{th} (13.4 mW cm^{-2}, Fig. S4a, ESI†). The TET efficiency was estimated to be 90.6% by the equation, $\Phi_{TET} = 1 - \Phi_P/\Phi_{P,0}$, where Φ_P and $\Phi_{P,0}$ are the donor phosphorescence quantum yields with and without the acceptor, respectively. TIPS-Nph showed a Φ_F of 71.0% at a concentration of 10 mM in hexyl benzoate (Fig. S5, ESI†). Substituting these values into eqn (1) yields an f value of 26.0%, which is close to that in THF (32%).[33] Note that this is the conservative estimation of the f value due to the inner filter effect and acceptor-to-donor back energy transfer.[36]

In order to evaluate the threshold excitation light intensity (I_{th}), an indicator for optimizing the TTA process, photoluminescence (PL) spectra were measured under different excitation intensities. The I_{th} value observed in hexyl benzoate was 13.4 mW cm^{-2}, about 5.8 times higher than 2.3 mW cm^{-2} in THF (Fig. S4a, ESI†).[33] TTA-UC occurs by molecular diffusion in solution and is also affected by solvent viscosity.[51,52] The viscosity of hexyl benzoate was measured as 4.54 cP at 25 °C, and the viscosity of THF was reported to be 0.46 cP at 25 °C.[53,54] The I_{th} in a solution can be expressed by the following equation,[55–57]

$$I_{th} = \frac{1}{8\pi a_0 \alpha \Phi_{ISC}\Phi_{TET} D_T \tau_T^2} \quad (2)$$

where a_0 is the effective distance of TTA, α is a donor absorption coefficient, D_T is a triplet diffusion constant, and τ_T is an acceptor triplet lifetime. The donor absorption in hexyl benzoate and THF showed no significant difference (Fig. S6, ESI†). The triplet diffusion constant can be considered as the molecular diffusion coefficient in solution and can be approximated

by the Stokes–Einstein equation,[58]

$$D_T = \frac{k_B T}{6\pi\mu R} \quad (3)$$

where k_B is the Boltzmann constant, T is temperature, μ is a solvent viscosity, and R is the molecular radius. The triplet lifetime τ_T of the acceptor was 1.83 and 0.88 ms in hexyl benzoate and THF, respectively (Fig. S4b, ESI†).[33] Using the experimental parameters and assuming that the effective distance on TTA (a_0) is independent of the solvent, it is predicted that I_{th} is 1.9 times higher in hexyl benzoate than in THF. This prediction is slightly different from the 5.8 times difference observed. While the exact reason for this difference is not clear at this moment, the effective triplet–triplet interaction might be different in different solvents.

We have developed a simple porous film impregnation method to create films that retain these excellent TTA-UC properties in solution. As a thin and porous film with good transparency in the UV and visible region, we used a polypropylene-based porous film with 38 μm thickness (Microporous Film, 3M). This porous film has a sponge structure, as indicated by the SEM images (Fig. S7, ESI†). The refractive index of polypropylene is 1.49,[59] which is similar to that of hexyl benzoate (1.49).[50] Due to the difference in refractive index between polypropylene and air (1.00),[60] the porous film was originally opaque, but it became transparent by being immersed in hexyl benzoate (Fig. 2a). This change of transparency occurred immediately after the immersion. The film thickness did not change with immersion in hexyl benzoate, and no significant swelling behavior was observed (Table S1, ESI†). Thermogravimetric analysis of the immersed porous film showed that 43 wt% hexyl benzoate was incorporated into the film. To characterize its TTA-UC properties, the porous film containing the hexyl benzoate solution of TIPS-Nph and $Ir(C6)_2(acac)$ was sandwiched between quartz substrates and sealed with epoxy resin in an argon-filled glovebox. Under the laser excitation of a wavelength at 445 nm, the film showed upconverted emission in the UV range (Fig. 2b). Note that the film showed an emission peak at 357 nm on the short-wavelength side, which was not observed in the bulk solution of TIPS-Nph and $Ir(C6)_2(acac)$ (Fig. S3a, ESI†). This appearance of the peak should be due to the reduction of self-absorption of acceptor emission by the shortening of the optical path length from 1 mm in the solution to 38 μm in the film. The TTA-UC efficiency of this film was obtained by the relative method using the phosphorescence of $Ir(C6)_2(acac)$ as an internal standard because the slight scattering nature of the film hampered the precise estimation of absorbance. Significantly, it showed the highest visible-to-UV TTA-UC efficiency η_{UC} of 27.6% as a film and a relatively low I_{th} of 20.4 mW cm^{-2} (Fig. 2b and c). The higher TTA-UC efficiency in the film than in the bulk solution is reasonable, considering the less reabsorption in the thinner sample geometry. The TTA-UC efficiency of the film becomes closer to the reported calculated value of 33.6% obtained by correcting for reabsorption based on the measured efficiency of 26.2%.[36] It was also found that continuous irradiation of the laser at 1.5 mW cm^{-2}, which corresponds to 1 sun (1.4 mW cm^{-2} for 445 ± 5 nm[61]), did not change the emission intensity for 60 min (Fig. S9, ESI†). To evaluate the storage stability of the film, TTA-UC measurements were performed after the film was left in the dark for 9 days. The I_{th} value of the film remained low at 29.1 mW cm^{-2} after storage (Fig. S10, ESI†). In future studies, it will be important to systematically examine how TTA-UC efficiency varies with pore size, film material, and film thickness in order to further optimize the TTA-UC properties in the thin film.

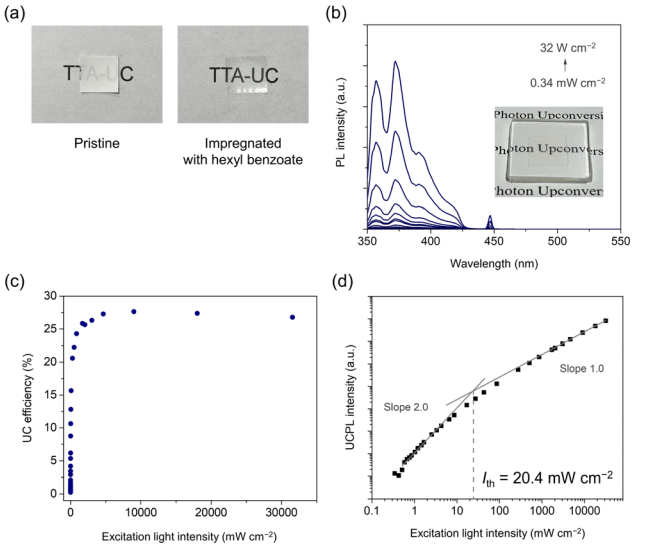

Fig. 2 (a) Photographs of a pristine porous film and a porous film impregnated with hexyl benzoate. (b) Photoluminescence (PL) spectra of the film at various excitation light intensities of a laser (445 nm) with a short-pass filter (425 nm). Inset is a photograph of the film sealed between quartz substrates. (c) Upconversion efficiencies and (d) upconversion PL intensities at 372 nm of the film in different excitation light intensities.

Taking advantage of the fact that the film created by the porous film impregnation method can be combined with any substrate, we have succeeded in utilizing even weaker light by combining it with a microlens array. Polymer lens arrays and microcavities were used to reduce the excitation light intensity which is required for efficient light upconversion.[62–65] In this study, a microlens array was used to focus the excitation light onto the film to reduce the threshold excitation light intensity (I_{th}). The porous film containing the hexyl benzoate solution was placed just below a microlens array (Fig. 3a). Microlenses are made of quartz and have a diameter of 124 μm and a pitch of 128 μm with a calculated focus diameter of *ca.* 3.0 μm (1708×) and a focus distance of 15–30 μm from the bottom of the microlens array. The thickness of the upconverting film is 38 μm, and thus the light can be focused inside the film.

Remarkably, when combined with the microlens array, the film's I_{th} value dropped below 0.60 mW cm^{-2}, corresponding to 0.43 sun (Fig. 3b and c). Because the I_{th} was too low, we could only observe up to a slope of 1.3 in our setup and not up to a slope of 2. Therefore, the actual I_{th} was too low to be determined in our setup and should be even lower than 0.60 mW cm^{-2}. Note that the linear region was observed from 8.7 mW cm^{-2}, suggesting that TTA occurs efficiently around the solar light intensity. Solutions showing visible-to-UV TTA-UC, which have been

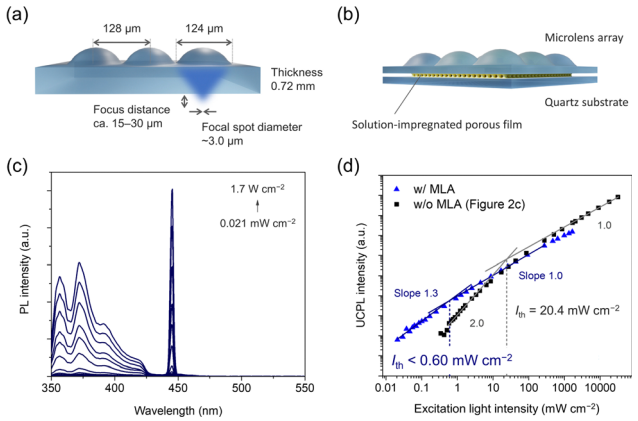

Fig. 3 Schematic illustration of (a) a microlens array and (b) a sandwiched sample structure. (c) PL spectra of the film integrated with the microlens array at various excitation light intensities of a laser (445 nm) with a short-pass filter (425 nm). (d) PL intensities at 372 nm of the film integrated with (blue triangle) and without (black square, the same data in Fig. 2c) microlens array (MLA) at different excitation intensities.

studied extensively, are not easy to combine with microlens arrays. Although conventional films can be easily combined with microlens arrays, obtaining efficient visible-to-UV TTA-UC in the form of films has been difficult. The newly developed porous film impregnation method can easily produce a film while maintaining the high TTA-UC efficiency of the solution and can be combined with microlens arrays to utilize the light of subsolar intensity.

Conclusions

We have developed the film showing the highest visible-to-UV TTA-UC efficiency of 27.6% to date and found a way to utilize subsolar light by combining it with the microlens array. The method of impregnating the porous film with the low-volatile upconversion solution is very simple and powerful, allowing the production of films that maintain the high TTA-UC performance of the solution. Moreover, we have demonstrated that the film can be combined with the microlens array to harvest subsolar-intensity light. This film would enable the generation of UV light from weak visible light including sunlight and room LED light towards various applications such as artificial photosynthesis, environmental purification, and water purification. Furthermore, the newly developed method is highly versatile and can be applied to other excitation wavelengths such as green, red, and near-infrared light by simply changing the type of dye.

Author contributions

N. H. and N. Y. conceived and designed the project. N. H., M. U., and B. S. carried out the experiments. N. H. and N. Y. wrote the manuscript with the input of M. U., B. S., and N. K.

Conflicts of interest

There are no conflicts to declare.

Acknowledgements

This work was partly supported by JSPS KAKENHI (JP20H02713, JP22K19051, JP20H05676, JP21J21739), the JST-FOREST Program (JPMJFR201Y), The Murata Science Foundation, Research Foundation for Opto-Science and Technology, and Kyushu University Platform of Inter-/Transdisciplinary Energy Research (Q-PIT) through its ''Module-Research Program''. We thank Ushio Inc. for providing the microlens array.

References

1 S. Baluschev, T. Miteva, V. Yakutkin, G. Nelles, A. Yasuda and G. Wegner, *Phys. Rev. Lett.*, 2006, **97**, 143903.
2 T. N. Singh-Rachford and F. N. Castellano, *Coord. Chem. Rev.*, 2010, **254**, 2560–2573.
3 J. Zhao, S. Ji and H. Guo, *RSC Adv.*, 2011, **1**, 937–950.
4 J.-H. Kim and J.-H. Kim, *J. Am. Chem. Soc.*, 2012, **134**, 17478–17481.
5 R. Andernach, H. Utzat, S. D. Dimitrov, I. McCulloch, M. Heeney, J. R. Durrant and H. Bronstein, *J. Am. Chem. Soc.*, 2015, **137**, 10383–10390.
6 V. Gray, D. Dzebo, M. Abrahamsson, B. Albinsson and K. Moth-Poulsen, *Phys. Chem. Chem. Phys.*, 2014, **16**, 10345–10352.
7 A. Monguzzi, R. Tubino, S. Hoseinkhani, M. Campione and F. Meinardi, *Phys. Chem. Chem. Phys.*, 2012, **14**, 4322–4332.
8 Y. C. Simon and C. Weder, *J. Mater. Chem.*, 2012, **22**, 20817–20830.
9 M. Wu, D. N. Congreve, M. W. B. Wilson, J. Jean, N. Geva, M. Welborn, T. Van Voorhis, V. Bulović, M. G. Bawendi and M. A. Baldo, *Nat. Photon.*, 2016, **10**, 31–34.
10 N. Yanai and N. Kimizuka, *Acc. Chem. Res.*, 2017, **50**, 2487–2495.
11 E. M. Gholizadeh, S. K. K. Prasad, Z. L. Teh, T. Ishwara, S. Norman, A. J. Petty II, J. H. Cole, S. Cheong, R. D. Tilley, J. E. Anthony, S. Huang and T. W. Schmidt, *Nat. Photon.*, 2020, **14**, 585–590.
12 S. P. Hill and K. Hanson, *J. Am. Chem. Soc.*, 2017, **139**, 10988–10991.
13 Z. Huang and M. L. Tang, *J. Am. Chem. Soc.*, 2017, **139**, 9412–9418.
14 C. J. Imperiale, P. B. Green, E. G. Miller, N. H. Damrauer and M. W. B. Wilson, *J. Phys. Chem. Lett.*, 2019, **10**, 7463–7469.
15 B. D. Ravetz, A. B. Pun, E. M. Churchill, D. N. Congreve, T. Rovis and L. M. Campos, *Nature*, 2019, **565**, 343–346.
16 J. M. Rowe, J. Zhu, E. M. Soderstrom, W. Xu, A. Yakovenko and A. J. Morris, *Chem. Commun.*, 2018, **54**, 7798–7801.
17 R. Sato, H. Kitoh-Nishioka, K. Kamada, T. Mizokuro, K. Kobayashi and Y. Shigeta, *J. Phys. Chem. Lett.*, 2018, **9**, 6638–6643.
18 S. Wieghold, A. S. Bieber, Z. A. VanOrman, L. Daley, M. Leger, J.-P. Correa-Baena and L. Nienhaus, *Matter*, 2019, **1**, 705–719.
19 X. Yang, J. Han, Y. Wang and P. Duan, *Chem. Sci.*, 2019, **10**, 172–178.

20 Q. Chen, Y. Liu, X. Guo, J. Peng, S. Garakyaraghi, C. M. Papa, F. N. Castellano, D. Zhao and Y. Ma, *J. Phys. Chem. A*, 2018, **122**, 6673–6682.
21 P. Duan, N. Yanai and N. Kimizuka, *Chem. Commun.*, 2014, **50**, 13111–13113.
22 V. Gray, P. Xia, Z. Huang, E. Moses, A. Fast, D. A. Fishman, V. I. Vullev, M. Abrahamsson, K. Moth-Poulsen and M. L. Tang, *Chem. Sci.*, 2017, **8**, 5488–5496.
23 S. He, X. Luo, X. Liu, Y. Li and K. Wu, *J. Phys. Chem. Lett.*, 2019, **10**, 5036–5040.
24 S. Hisamitsu, J. Miyano, K. Okumura, J. K.-H. Hui, N. Yanai and N. Kimizuka, *ChemistryOpen*, 2020, **9**, 14–17.
25 X. Jiang, X. Guo, J. Peng, D. Zhao and Y. Ma, *ACS Appl. Mater. Interfaces*, 2016, **8**, 11441–11449.
26 Y. Kawashima, H. Kouno, K. Orihashi, K. Nishimura, N. Yanai and N. Kimizuka, *Mol. Syst. Des. Eng.*, 2020, **5**, 792–796.
27 K. Okumura, N. Yanai and N. Kimizuka, *Chem. Lett.*, 2019, **48**, 1347–1350.
28 J. Peng, X. Guo, X. Jiang, D. Zhao and Y. Ma, *Chem. Sci.*, 2016, **7**, 1233–1237.
29 B. Pfund, D. M. Steffen, M. R. Schreier, M. S. Bertrams, C. Ye, K. Börjesson, O. S. Wenger and C. Kerzig, *J. Am. Chem. Soc.*, 2020, **142**, 10468–10476.
30 T. N. Singh-Rachford and F. N. Castellano, *J. Phys. Chem. A*, 2009, **113**, 5912–5917.
31 N. Yanai, M. Kozue, S. Amemori, R. Kabe, C. Adachi and N. Kimizuka, *J. Mater. Chem. C*, 2016, **4**, 6447–6451.
32 W. Zhao and F. N. Castellano, *J. Phys. Chem. A*, 2006, **110**, 11440–11445.
33 N. Harada, Y. Sasaki, M. Hosoyamada, N. Kimizuka and N. Yanai, *Angew. Chem., Int. Ed.*, 2021, **60**, 142–147.
34 M. Uji, N. Harada, N. Kimizuka, M. Saigo, K. Miyata, K. Onda and N. Yanai, *J. Mater. Chem. C*, 2022, **10**, 4558–4562.
35 Y. Murakami, A. Motooka, R. Enomoto, K. Niimi, A. Kaiho and N. Kiyoyanagi, *Phys. Chem. Chem. Phys.*, 2020, **22**, 27134–27143.
36 A. Olesund, J. Johnsson, F. Edhborg, S. Ghasemi, K. Moth-Poulsen and B. Albinsson, *J. Am. Chem. Soc.*, 2022, **144**, 3706–3716.
37 T. J. B. Zähringer, M.-S. Bertrams and C. Kerzig, *J. Mater. Chem. C*, 2022, **10**, 4568–4573.
38 B. Yurash, A. Dixon, C. Espinoza, A. Mikhailovsky, S. Chae, H. Nakanotani, C. Adachi and T.-Q. Nguyen, *Adv. Mater.*, 2022, **34**, 2103976.
39 M. Barawi, F. Fresno, R. Pérez-Ruiz and V. A. de la Peña O'Shea, *ACS Appl. Energy Mater.*, 2018, **2**, 207–211.
40 F. Glaser, C. Kerzig and O. S. Wenger, *Chem. Sci.*, 2021, **12**, 9922–9933.
41 T. J. B. Zähringer, J. A. Moghtader, M.-S. Bertrams, B. Roy, M. Uji, N. Yanai and C. Kerzig, *Angew. Chem., Int. Ed.*, 2023, **62**, e202215340.
42 A. J. Svagan, D. Busko, Y. Avlasevich, G. Glasser, S. Baluschev and K. Landfester, *ACS Nano*, 2014, **8**, 8198–8207.
43 M. Kinoshita, Y. Sasaki, S. Amemori, N. Harada, Z. Hu, Z. Liu, L. K. Ono, Y. Qi, N. Yanai and N. Kimizuka, *ChemPhotoChem*, 2020, **4**, 5271–5278.
44 R. Vadrucci, A. Monguzzi, F. Saenz, B. D. Wilts, Y. C. Simon and C. Weder, *Adv. Mater.*, 2017, **29**, 1702992.
45 P. Bharmoria, S. Hisamitsu, Y. Sasaki, T. S. Kang, M.-A. Morikawa, B. Joarder, K. Moth-Poulsen, H. Bildirir, A. Mårtensson, N. Yanai and N. Kimizuka, *J. Mater. Chem. C*, 2021, **9**, 11655–11661.
46 T. Kashino, R. Haruki, M. Uji, N. Harada, M. Hosoyamada, N. Yanai and N. Kimizuka, *ACS Appl. Mater. Interfaces*, 2022, **14**, 22771–22780.
47 P. B. Merkel and J. P. Dinnocenzo, *J. Lumin.*, 2009, **129**, 303–306.
48 R. Enomoto and Y. Murakami, *J. Mater. Chem. C*, 2023, **11**, 1678–1683.
49 F. Saenz, A. Ronchi, M. Mauri, D. Kiebala, A. Monguzzi and C. Weder, *ACS Appl. Mater. Interfaces*, 2021, **13**, 43314–43322.
50 R. L. Merker and M. J. Scott, *J. Org. Chem.*, 1961, **26**, 5180–5182.
51 V. R. Nicholas J. Turro and J. C. Scaiano, *Modern Molecular Photochemistry of Organic Molecules*, University Science Books, Sausalito, California, 2010.
52 Y. Murakami and K. Kamada, *Phys. Chem. Chem. Phys.*, 2021, **23**, 18268–18282.
53 S. Rodríguez, C. Lafuente, P. Cea, F. M. Royo and J. S. Urieta, *J. Chem. Eng. Data*, 1997, **42**, 1285–1289.
54 C. Carvajal, K. J. Tölle, J. Smid and M. Szwarc, *J. Am. Chem. Soc.*, 1965, **87**, 5548–5553.
55 A. Monguzzi, J. Mezyk, F. Scotognella, R. Tubino and F. Meinardi, *Phys. Rev. B: Condens. Matter Mater. Phys.*, 2008, **78**, 195112.
56 Y. Y. Cheng, T. Khoury, R. G. C. R. Clady, M. J. Y. Tayebjee, N. J. Ekins-Daukes, M. J. Crossley and T. W. Schmidt, *Phys. Chem. Chem. Phys.*, 2010, **12**, 66–71.
57 A. Haefele, J. Blumhoff, R. S. Khnayzer and F. N. Castellano, *J. Phys. Chem. Lett.*, 2012, **3**, 299–303.
58 P. W. Atkins and J. De Paula, *Atkins' Physical Chemistry*, Oxford University Press, Oxford, 10th edn, 2014.
59 D. W. van Krevelen, *Properties of Polymers: Their Correlation With Chemical Structure; Their Numerical Estimation and Prediction from Additive Group Contributions*, Elsevier, Amsterdam, London, New York, Tokyo, 3rd completely rev. edn, 1990.
60 P. E. Ciddor, *Appl. Opt.*, 1996, **35**, 1566–1573.
61 Reference Air Mass 1.5 Spectra (ASTM G-173-03), **https://www.nrel.gov/grid/solar-resource/spectra-am1.5.html**, (accessed September 26th, 2022).
62 D. Polak, R. Jayaprakash, T. P. Lyons, L. Á. Martínez-Martínez, A. Leventis, K. J. Fallon, H. Coulthard, D. G. Bossanyi, K. Georgiou, A. J. Petty II, J. Anthony, H. Bronstein, J. Yuen-Zhou, A. I. Tartakovskii, J. Clark and A. J. Musser, *Chem. Sci.*, 2020, **11**, 343–354.
63 M. Wu, T.-A. Lin, J. O. Tiepelt, V. Bulović and M. A. Baldo, *Nano Lett.*, 2021, **21**, 1011–1016.
64 Q. Liu, H. Liu, D. Li, W. Qiao, G. Chen and H. Ågren, *Nanoscale*, 2019, **11**, 14070–14078.
65 L. Liang, D. B. L. Teh, N.-D. Dinh, W. Chen, Q. Chen, Y. Wu, S. Chowdhury, A. Yamanaka, T. C. Sum, C.-H. Chen, N. V. Thakor, A. H. All and X. Liu, *Nat. Commun.*, 2019, **10**, 1391.

